Materials Science and Engineering B 301 (2024) 117147

Contents lists available at ScienceDirect

Materials Science & Engineering B

journal homepage: www.elsevier.com/locate/mseb

Sustainable solutions for clean water: Green synthesized Cu-Ag-Bimetallic nanoparticles based nano catalyst

Parvathalu Kalakonda [a,*], Anusha Bashitangu [a], Pritam Mandal [c], Sarvani Jowhar Khanam [b], Murali Banovath [b], Imran Hasan [d], Bala Bhaskar Podila [a]

[a] Department of Physics, Government City College (A), Nayapul, Osmania University, Hyderabad, Telangana 500002, India
[b] Department of Chemistry, University of Hyderabad, Hyderabad 500046, India
[c] Department of Physics, Michigan Technological University, Houghton, MI 49931, USA
[d] Department of Chemistry, College of Science, King Saud University, Riyadh-11451, KSA

ARTICLE INFO

Keywords:
Bimetallic Nanoparticles
Green synthesis
Argyreia Nervosa
Photocatalytic activity

ABSTRACT

The green synthesis of copper (Cu)-silver (Ag) bimetallic nanoparticles (Cu-Ag BMNPs) using Argyreia nervosa (AN) plant leaf extract as a dual reducing and stabilizing agent is an eco-friendly and sustainable method with significant potential for diverse photo-catalytic applications. This study explores the photo-catalytic activity of biosynthesized Cu-Ag-BMNPs employing methylene blue (MB) dye under visible light. FTIR analysis reveals bio-functional groups and chemical bands, while SEM and XRD analyses provide morphological and structural details. UV–Vis spectroscopy indicates absorption peaks at 300–350 nm for CuNPs, 350–550 nm for AgNPs, and 400–550 nm for Cu-Ag-BMNPs, with an optical band gap of 3.6 eV. The results demonstrate an 85% dye degradation rate, underscoring the efficiency of Cu-Ag-BMNPs as photo-catalysts for environmentally friendly remediation. We assessed the rate constant governing the degradation of MB dye by Cu-Ag-BMNPs, employing the pseudo-first-order kinetics model. This green synthesis approach not only minimizes hazardous chemical use but also leverages the inherent bioactive properties of the plant extract, showcasing promise in addressing water pollution through organic contaminant removal.

1. Introduction

The swift advancement in technological modernization and industrialization has led to the release of industrial effluents and organic dyes into aquatic ecosystems [1–5]. These dyes widely used in industries like textiles, cosmetics, and pharmaceuticals, also pose health risks to humans, including skin diseases and cancer [6–9]. Addressing dye contamination in aquatic ecosystem is crucial, researchers have developed methods like ion exchange, chemical oxidation, and photocatalysis to combat dye pollution [10–14]. Photocatalytic degradation, using metal nanoparticles as catalysts, offers an eco-friendly solution [15,16]. It breaks down dyes into harmless byproducts, safeguarding water ecosystems and human health. This eco-friendly method underscores the importance of adopting environmentally responsible industrial practices in our conscientious world.

To effectively degrade organic dyes in water bodies, it is imperative to employ metal nanomaterials with a substantial surface area-to-volume ratio [20,21]. Among these materials, metal nanoparticles (MNPs), including CuNPs, ZnNPs, and AgNPs, stand out as promising photo-catalysts, particularly in the presence of sunlight, owing to their energy band gap [22–25]. Copper oxide (CuO) is a noteworthy semiconductor characterized by its small range of band gap, which typically falls within the range of 2.0 to 2.7 eV (eV) [26]. This unique property renders CuNPs highly responsive and efficient in optical and photocatalytic applications [27,28]. Consequently, Cu-Ag BMNPs exhibit significant potential in the realm of dye degradation in aqueous environments.

In the pursuit of environmentally friendly solutions, the eco-friendly green synthesis of BMNPs utilizing plant extract has emerged as the optimal green synthesis method [29–31]. Building upon our prior research on MNPs [34,35], this present study employs a green synthesis method to create Cu-Ag BMNPs nanocomposite using AN leaf extract. Subsequently, we assess the efficacy of these synthesized Cu-Ag BMNPs in degrading Methylene Blue (MB) dye when exposed to sunlight. The main objective of this paper revolves around the environmentally friendly synthesis of Cu-Ag BMNPs and their potential applications for

* Corresponding author.
E-mail address: parvathalu.k@gmail.com (P. Kalakonda).

https://doi.org/10.1016/j.mseb.2023.117147
Received 26 October 2023; Received in revised form 2 December 2023; Accepted 25 December 2023
Available online 28 December 2023

mitigating water pollutants, including a range of dyes. Through this study, we aim to gain insights into the environmental photocatalytic properties of the newly synthesized materials. By exploring the potential of these nanoparticles, we contribute to the ongoing efforts to develop sustainable solutions for tackling water pollution, underscoring the importance of environmentally conscious practices in scientific research and innovation.

Metal nanoparticles are highly valued in the field of nanotechnology due to their multifaceted properties stemming from their nanoscale size and exceptional surface area-to-volume ratio, encompassing optical, electrical, catalytic, magnetic, and antimicrobial characteristics [40–43]. Bimetallic nanoparticles, exemplified by copper-silver (Cu-Ag) variants, stand out within this category. They feature a core–shell nanostructure, enhancing their multifunctional attributes through the synergistic interaction of their constituent metal ions. Notably, while Argyreia Nervosa (AN) plant leaf extract has been employed for mono-metallic nanoparticle synthesis, its potential for creating copper-silver bimetallic nanoparticles (Cu-Ag BMNPs) remains untapped. The AN plant is celebrated for its therapeutic qualities, encompassing anti-inflammatory and stress-reducing properties. Thus, exploring AN plant extract for green Cu-Ag BMNP synthesis is an intriguing venture, bridging the plant's therapeutic legacy with the exciting realm of advanced nanomaterials.

Catalysis assumes a central role in the realm of dye degradation and water purification, wielding substantial influence over environmental remediation initiatives. Fig. 1 illustrates schematic depicting water purification through dye degradation using metal nanoparticles. The vast economic impact of catalysis-based industries, potentially generating trillions of dollars in annual commodities [36,37], underscores its global significance. Chemical and pharmaceutical industries primarily prefer heterogeneous catalysis because of its benefits, such as the ease of separating the catalyst, its durability, suitability, and sustainability for their continuous easy operations. However, the design of catalyst materials remains a challenging endeavor due to the complex nature of their structure and limited comprehension of their active centers. Extensive research is dedicated to innovative catalyst design [38,39], crucial for consistent mass production meeting industrial demands [40–42]. Metal nanoparticles emerge as promising catalyst candidates, addressing both qualitative and quantitative aspects of global demand. Their unique properties and versatility position them at the forefront of catalysis research, promising to redefine efficient and sustainable industrial processes [40–45].

This study represents a pioneering effort in utilizing AN leaf extract as a dual-function reducing and stabilizing agent in the synthesis of Cu-Ag BMNPs. Our green synthesis approach not only highlights its potential for large-scale Cu-Ag BMNP production but also emphasizes its energy-efficient and cost-effective nature for commercial applications. Cu-Ag BMNPs were then employed as catalysts to assess their photocatalytic prowess in dye degradation, revealing their superior performance in this regard. These findings signify the promising role of Cu-Ag BMNPs in enhancing photo-catalytic processes, with significant implications for environmental remediation and wastewater treatment.

2. Materials and methodology

2.1. Materials

We obtained Copper (II) Oxide and Silver nitrate (99 % high purity), and methylene blue dye, all solvents, with research grade (99 %), from Sigma-Aldrich in Bangalore, India. The leaves of the Aegyreia nervosa plant were collected from Medicinal Plants Garden, Hyderabad.

2.2. Synthesis of Cu-Ag-BMNPs

The Argyreia nervosa foliage underwent a meticulous cleansing with deionized, DI, water to eliminate any contaminants. Following this, the surface moisture of the leaves was allowed slowly to evaporate at a room temperature, and the leaves were then finely ground into tiny powder of particles. Next, 2 g of AN material were blended with 50 ml of DI water and agitated at 75 °C for a duration of 15–20 min. The resultant AN extract was subsequently separated using filter paper and subjected to centrifugation for 25 min

To Cu-Ag BMNPs, we employed a precise procedure. Initially, 50 ml of AN leaf extract were slowly introduced drop by drop (at a rate of one drop per second) into a 200 ml beaker containing a 20 % weight/volume solution of CuO and AgNO3. This mixture was prepared and maintained at a controlled temperature of 90 °C, while it was vigorously stirred for 20 min at 600 revolutions per minute (rpm). The AN extract was added from the high-quality burette with careful control to maintain a uniform rate, while the resultant composite mixture was consistently agitated at a speed of 500–600 rpm. The synthesis procedure was prolonged until a noticeable shift in the color of the reaction mixture became observable. Subsequently, the solution underwent centrifugation at 4000 rpm for duration of 20–25 min, and the resulting residue was dried in an oven maintained at 60 °C, resulting in the formation of a solid powder. For a visual representation of the complete synthesis procedure and the

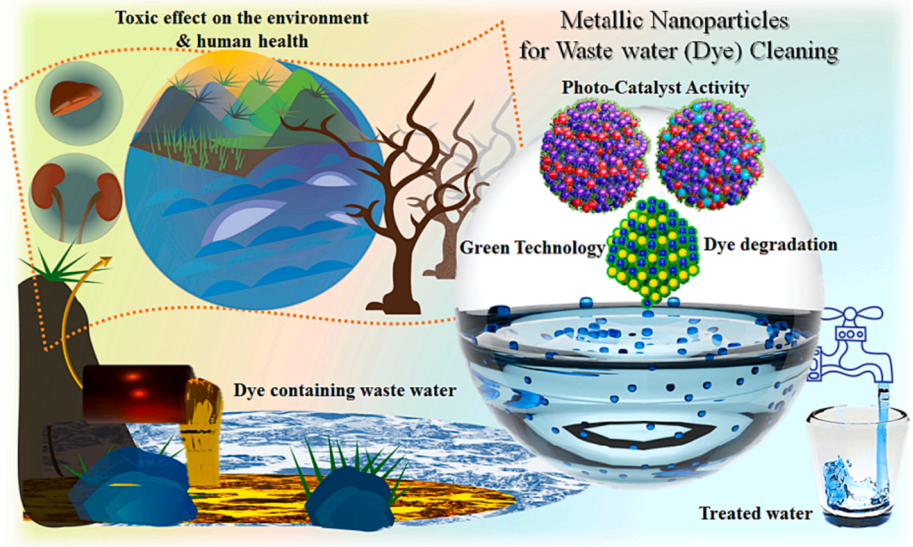

Fig. 1. Schematic of purification of water via dye degradation activity using bimetallic nanoparticles (Cu-Ag BMNPs).

schematic mechanism behind Cu-Ag-BMNPs, please refer to Fig. 2.

2.3. Characterization of Cu-Ag BMNPs

The formation of Cu-Ag BMNPs was verified through UV–Vis spectroscopy (UVJASCO V-750 spectrometer), specifically by observing the SPR phenomenon. This UV–Vis analysis enabled the identification of the synthesized Cu-Ag BMNPs based on their distinctive absorption peaks.

To discern the precise phytochemical groups accountable for the creation of metallic nanoparticles (MNPs), Fourier Transform Infrared Spectroscopy (FTIR: IR Thermo Fisher Nicolet iS5) was harnessed. The samples underwent analysis utilizing an IR-Thermo Fisher Nicolet iS5 spectrometer, capturing spectra within the range of 400 to 4000 cm^{-1}. We utilized FTIR spectroscopy to obtain valuable information regarding the functional groups and chemical bonds involved in stabilizing and capping the Cu-Ag BMNPs.

To delve into the surface details and grain dimensions of the synthesized Cu-Ag BMNPs, we employed SEM. Thin Cu-Ag BMNPs films were crafted on grids, meticulously scrutinized using the ZEISS Merlin Compact instrument operated at an accelerated voltage of 20 k. Through SEM graphical analysis using image J software, we attained a visual depiction of the BMNPs, facilitating the precise measuring of their grain size distribution and surface inherent details.

To scrutinize the Cu-Ag BMNPs crystal structure, we employed X-Ray Diffraction (XRD) with a state of the Bruker D8 Advance Instrument. This technique furnished essential insights into the crystalline phases and crystallographic arrangement of the synthesized nanoparticles. The XRD patterns were acquired utilizing Cu-Kα radiation, allowing us to decipher the intricate details of the Cu-Ag-BMNPs' structural characteristics. In summary, employing UV–vis spectroscopy, FTIR analysis, SEM imaging, and XRD measurements facilitated a comprehensive characterization of the Cu-Ag BMNPs that was inclusive of evaluating their photocatalytic performance, material attributes like optical properties, chemical composition, structural morphology, and crystalline arrangement.

2.4. Photocatalytic activity

To evaluate the photo-catalytic activity of the Cu-Ag BMNPs in degrading methylene blue (MB) dye, a visible light source was employed as a substitute for natural sunlight. The reaction commenced with the addition of a 5 ml/3ml solution of Cu-Ag BMNPs catalyst with a concentration of 10 mg/ml into a 40 ml dye solution. The resulting solution was stirred in a darkroom for 20 min to establish the adsorption process. To monitor the progress of the reaction, samples were collected at 30-minute intervals, and their absorption peaks were analyzed using UV–Vis spectroscopy with desirable conditions. The initial UV–Vis spectra data were obtained for the MB dye, displaying characteristic bands at 630 nm and 430 nm. Under visible light irradiation, the solution was continuously stirred, and 3 ml of suspension was withdrawn at 30-minute intervals for up to 3 hrs to track changes in the MB dye absorption peak. Dye degradation was quantified using the following equation [46], utilizing UV–Vis spectrum data.

$$\text{Degradation } (\%) = \left(\frac{A_0 - A_t}{A_0}\right) \times 100$$

Where A_0 represents the initial absorption at time t = 0, and A_t represents the absorption at a later time t.

3. Results and discussion

3.1. Scanning electron microscopy

We utilized SEM to scrutinize the surface details of the Cu-Ag BMNPs, as illustrated in Fig. 3. The SEM micrograph of the Cu-Ag-BMNPs unveiled an array of irregular-shaped structures spanning sizes from 100 to 500 nm. In contrast, the AgNPs exhibited well-defined spherical forms, with an average size spanning from approximately 30 to 50 nm. Intriguingly, the SEM of Cu-Ag BMNPs morphology showcased the formation of irregular clusters characterized by rough surfaces and varying sizes. This aggregation of clusters may be attributed to the diverse crystallization growth patterns of CuNPs and AgNPs during synthesis.

3.2. Fourier transform infrared spectroscopy

The FTIR analysis provided insights into the functional groups and chemical bands within the synthesized CuNPs, AgNPs, and Cu-Ag

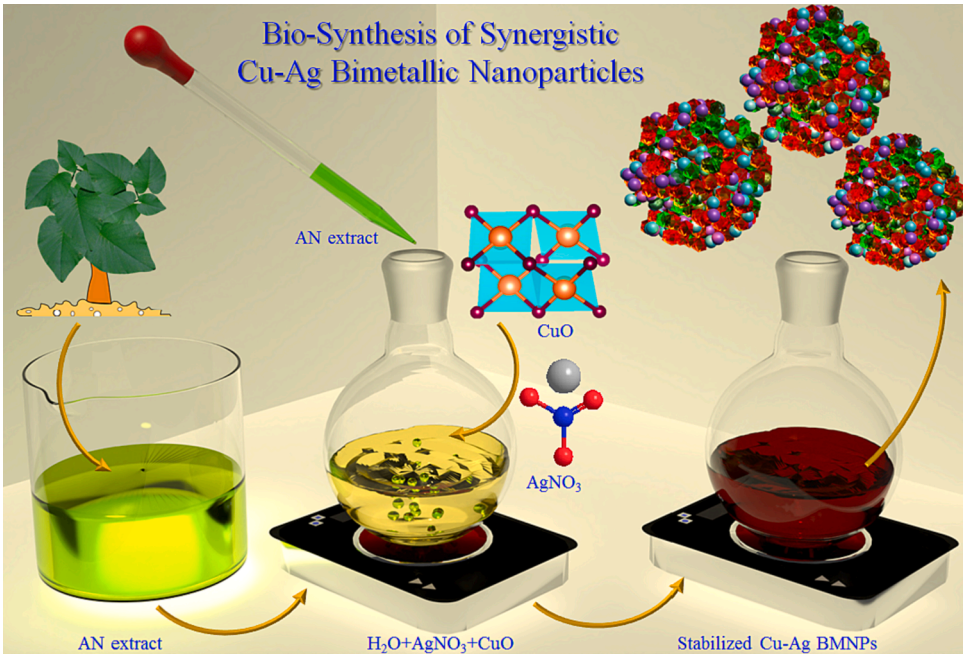

Fig. 2. Synthesis process of Cu-Ag BMNPs.

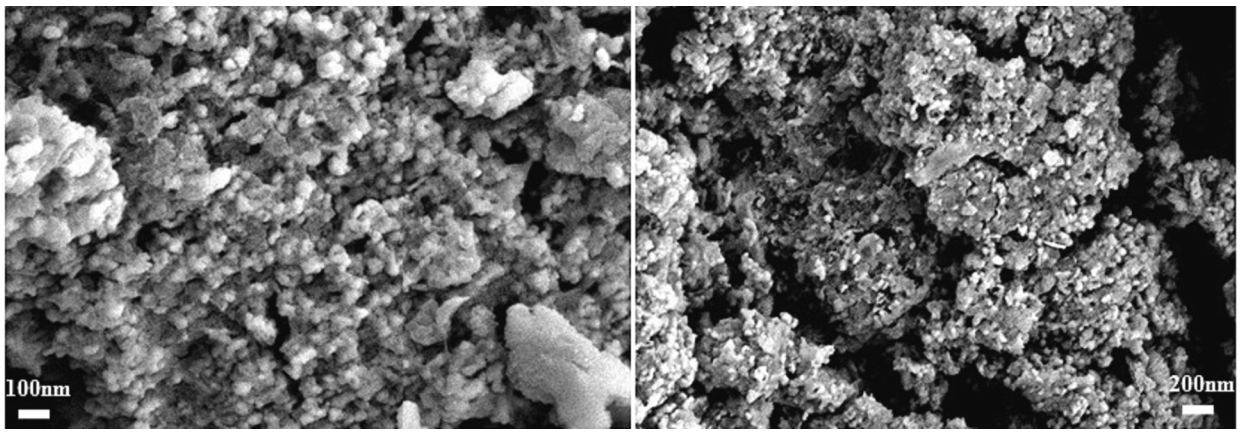

Fig. 3. SEM micrographs of Cu-Ag-BMNPs.

BMNPs nanomaterials. The FTIR spectra, as illustrated in Fig. 4, revealed the distinct presence of specific biomolecules responsible for reducing Cu, Ag, and bimetallic, BM, ions while stabilizing the Cu-Ag BMNPs. Comparing these observed peak values allowed us to identify the surface functional groups. Notably, the peak at 496 cm^{-1} indicated stretching vibrations associated with the Cu–O bond, while the peaks at 1628 cm^{-1} were attributed to N–H stretching vibrations and C-N/C–C stretching, signifying the presence of proteins. Additionally, the peak at 3308 cm^{-1} suggested the existence of phenolic compounds in the leaf extract, which played a crucial role in the synthesis and formation of CuNPs, and Cu-Ag BMNPs. Importantly, the FTIR spectrum confirmed the absence of surfactants on the Cu-Ag BMNPs' surface, underscoring the purity of the synthesized Cu-Ag BMNPs.

3.3. UV–VIS spectroscopy analysis

The optical characteristics of Cu-Ag BMNPs are intricately affected by factors encompassing surface details such as grain size, and shape. Within our investigation, we scrutinized the UV–Vis spectroscopy analysis of the synthesized AgNPs, CuNPs, and Cu-Ag bimetallic nanoparticles (Cu-Ag BMNPs) to ascertain the intensity of absorption peaks attributed to Surface Plasmon Resonance (SPR). During this analysis, we observed broad absorption peaks spanning distinct wavelength ranges: 300 to 350 nm for CuNPs, 350 to 550 nm for AgNPs, and 400 to 550 nm for Cu-Ag-BMNPs. Remarkably, the breadth of these peaks expanded notably with higher Cu content within the Cu-Ag BMNPs composite. Furthermore, we meticulously recorded and presented the maximum absorption peaks in Fig. 5 for comprehensive visualization.

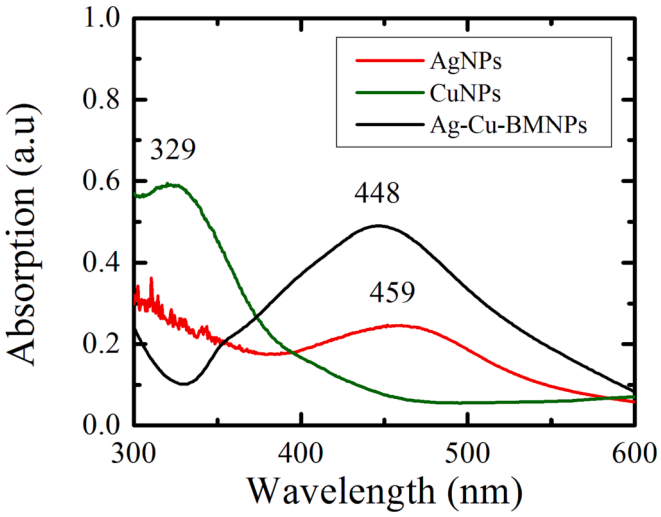

Fig. 5. UV–Vis Absorption spectroscopy of AgNPs, CuNPs and Cu-Ag-BMNPs.

3.4. X-RAY diffraction (XRD) analysis

XRD analysis, facilitated by X'pert High Score Plus software, played a pivotal role in unraveling the crystalline details of the Cu-Ag BMNPs nanocomposite. The XRD patterns unveiled a noteworthy revelation: the as-synthesized Cu-Ag BMNPs exhibited nanocomposite crystalline structures devoid of any impurities. Fig. 6 showcased the diffraction

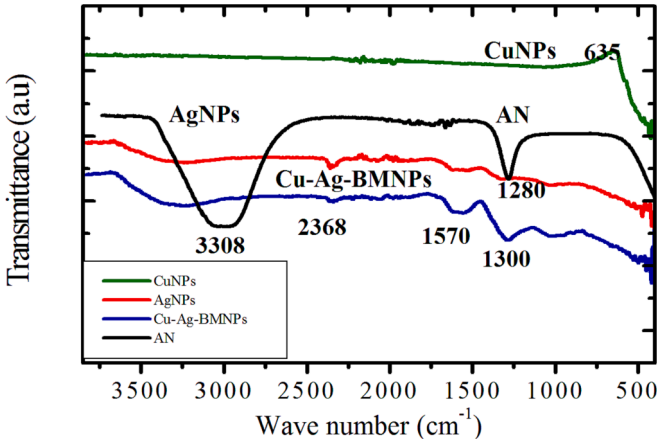

Fig. 4. FTIR spectrum of AgNPs, CuNPs and Cu-Ag-BMNPs.

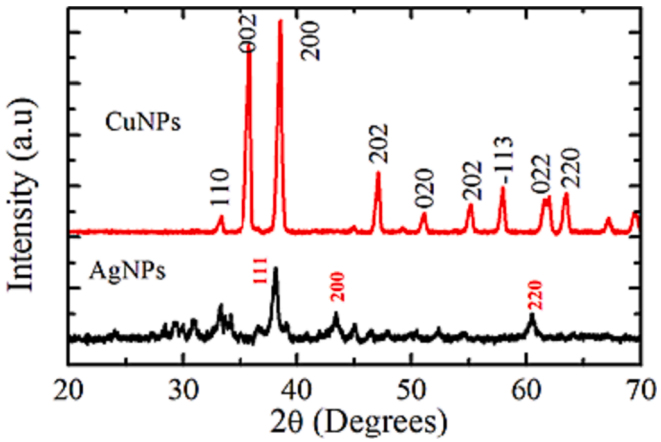

Fig. 6. XRD spectrum of CuNPs and AgNPs.

pattern of individual CuNPs and AgNPs, while Fig. 7 depicted the hybrid BMNPs' composite XRD spectrum. Notably, the XRD pattern of Cu-Ag BMNPs revealed wider peaks, affirming the polycrystalline nature of the synthesized BMNPs. Scherer's equation was harnessed to know the crystal size for Cu-Ag BMNPs. The results revealed strong peak intensities at specific angles, specifically at 37.5^0, 45.6^0, 64^0, and 77^0 degrees. These findings strongly indicate the existence of a crystalline grain phase within Cu-Ag BMNPs. Moreover, the confirmation of reflection planes aligning with (111), (200), (220), and (311) serves as additional evidence substantiating the crystalline character of Cu-Ag BMNPs. The most prominent peak, notably at (111), facilitated precise determination of the lattice constant using the following equation.

$$a = \lambda\left(\frac{\sqrt{h^2+k^2+l^2}}{2\sin\theta}\right)A^0$$

The crystalline grain size of the Cu-Ag BMNPs was computed utilizing Debye-Scherr's equation: $D = 0.9\lambda / \beta\cos\theta$. In this context, λ denotes the wavelength of X-ray radiation utilized in XRD, β represents the full width at half maximum, and 2θ corresponds to the diffraction angle. The analysis yielded an estimated nanoparticle crystalline size of approximately 25 nm. The reduction process of the precursor CuO and $AgNO_3$ salt solution commences immediately upon the addition of even a few drops of leaf extract solution, as evidenced by the noticeable change in the solution's color. In this complex transformation, the bio-phytochemicals naturally present in the AN leaf extract play a pivotal key role in the reduction, capping, and stabilization of the BMNPs composite. In the course of this intriguing process, the conversion from enol to keto bio-flavonoid molecules triggers the liberation of hydrogen (H) atoms. This liberation, in turn, plays a pivotal role in expediting the reduction of Cu and Ag metal ions, ultimately giving rise to the formation of the Cu-Ag-BMNPs composite. Although the precise mechanism governing Cu-Ag-BMNPs synthesis via plant leaf extract remains elusive, it is theorized that the color shift observed around 30 to 40 min into the process may be attributed to oxidation, a crucial factor driving the synthesis of Cu-Ag-BMNPs. Additionally, electrostatic attractions likely play a pivotal role in binding metal oxide ions together, thereby fostering the formation of stabilized nanoparticles and inhibiting the aggregation of Cu-Ag-BMNPs clusters. Despite the ongoing quest for a comprehensive understanding of the metal nanoparticle synthesis mechanism, the undeniable contribution of plant leaf extracts in crafting Cu-Ag-BMNPs underscores the significance of biogenic green synthesis. This approach holds immense potential, lauded for its eco-friendliness, non-toxicity, and cost-effectiveness. This avenue of research offers immense promise for scientists dedicated to advancing sustainable and environmentally responsible nanoparticle synthesis.

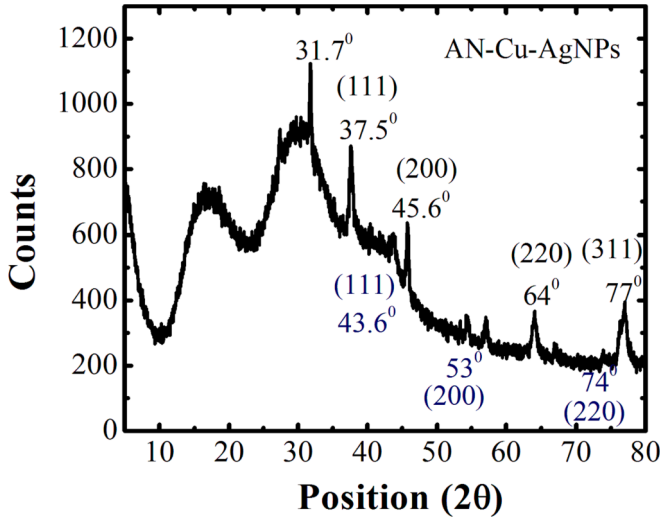

Fig. 7. XRD spectrum of Cu-Ag-BMNPs.

3.5. Evaluation of Photo-Catalytic activity of Cu-Ag-BMNPs

Fig. 8 visually illustrates the photo-catalytic performance of Cu-Ag-BMNPs in the degradation of MB dye. The rate of dye degradation hinges on several crucial variables, encompassing the duration of irradiation, the type of light source utilized, as well as the concentrations of both the dye and the catalyst. In our study, sunlight played the central role as the primary light source driving the degradation process. Notably, the impressive band gap and the substantial surface area to volume ratio of Cu-Ag-BMNPs exert a profound influence on their catalytic efficacy in the degradation of dyes. We methodically obtained samples at designated time intervals subsequent to exposure to light, and their characterization was carried out through the analysis of absorption spectra using UV–Vis spectroscopy. Our research findings unveiled a reduction in the intensity of the absorption band as the duration of light exposure increased. To offer a comprehensive perspective, we have thoughtfully presented the extent of dye absorption in the presence of Cu-Ag-BMNPs in Fig. 8 **and** Fig. 9, illustrating the impact of two different concentrations (3 ml & 5 ml) of Cu-Ag-BMNPs catalyst on the degradation process.

The Cu-Ag BMNPs composite nano-catalyst plays a significant role in reducing MB dye, resulting in a substantial decrease in absorption from 0.5 to 0.1 for a 3 ml Cu-Ag BMNPs catalyst. Conversely, a lower absorption is observed for a 5 ml Cu-Ag BMNPs catalyst at a 25μLt MB dye concentration (Fig. 9).

The optical band gap of Cu-Ag BMNPs, initially established about 3.6–3.8 eV for both concentration of Cu-Ag BMNPs catalyst through UV data analysis, was subsequently corroborated using the Tauc relation and absorption spectrum [47–49], as illustrated in Fig. 10. This substantial band gap underscores the promising potential of Cu-Ag BMNPs as potent photo-catalysts for diverse applications. The wide band gap facilitates the efficient utilization of visible light in catalytic processes, thus enhancing their higher photo-catalytic activity. This study underscores the prospective environmental applications of Cu-Ag BMNPs in the realm of advanced materials science and catalysis.

The degradation or decolonization of dyes is primarily attributed to the action of oxygen radicals and hydroxyl radicals, both of which play a crucial role in breaking down and neutralizing toxic contaminants present in the dye. As the exposure time to light increases, the color of MB dye gradually transitions into a lighter shade of blue or becomes colorless. The degradation efficiency for MB dye, quantified at approximately 85 % and 70 % for two different concentrations (3 ml, 5 ml) of Cu-Ag BMNPs catalyst (Fig. 11). The degradation efficiency was noted after approximately 2 h of exposure to a 10-watt light source, employing both 3 ml and 5 ml of the Cu-Ag-BMNPs photo-catalyst. Significantly, a higher degradation rate was observed at the lower concentration of 3 ml of the Cu-Ag-BMNPs catalyst after two hours, suggesting an optimal catalyst concentration for the reduction process. This observation highlights the complex dynamics involved in the photo-catalytic degradation of dyes, providing valuable insights for further scientific exploration.

3.5.1. Kinetic studies of biogenic Cu-Ag-BMNPs

To assess the photo-catalytic efficiency and kinetics of MB dye degradation facilitated by the Cu-Ag-BMNPs catalyst, we utilized the first-order kinetic theory model. The model is represented as follows

$$\ln\left(\frac{A_0}{A_t}\right) = kt \quad (1)$$

Certainly, in the equation outlined, A_0 indicates the MB dye absorption value at the initial time t = 0, A_t represents the MB dye absorption at time t, and k stands for the rate constant value. Our study extensively

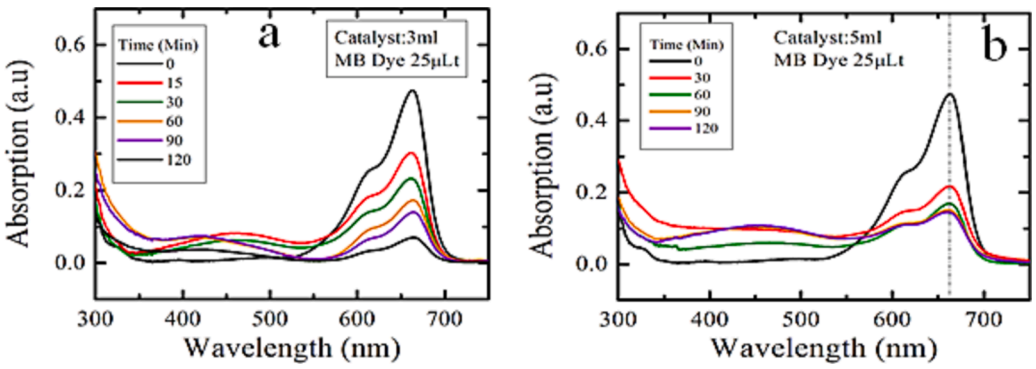

Fig. 8. Photocatalytic activity of Cu-Ag-BMNPs with Catalyst (a) 3 ml, (b) and 25 µLt of MB dye (200 ml DI water).

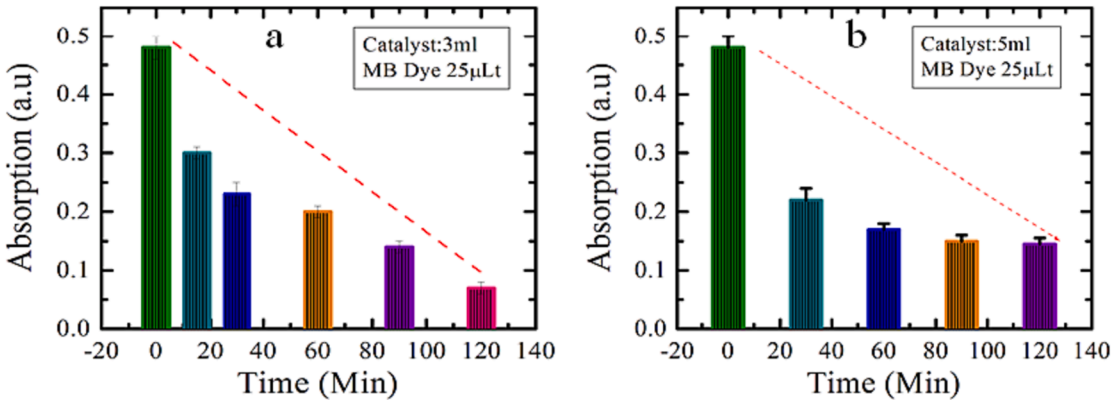

Fig. 9. Absorption of MB dye as the function time (Min) at (a) 3 ml, (b) 5 ml Catalyst concentration.

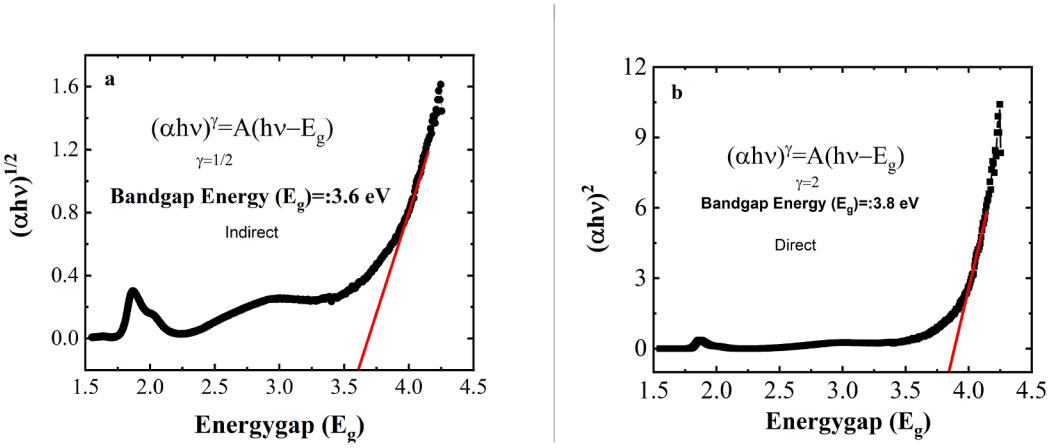

Fig. 10. Photocatalytic activity of Cu-Ag-BMNPs with Catalyst 5 ml and 25 µLt of MB dye (200 ml DI water).

explored the kinetics of MB dye photo-degradation catalyzed by Cu-Ag-BMNPs, and the resultant findings are effectively illustrated in Fig. 12 **(a)** $\left(\ln\left(\frac{A_0}{A_t}\right)\right.$ versus time) at 5 ml catalyst. We conducted a comprehensive investigation into the kinetic photo-degradation of MB dye using Cu-Ag-BMNPs, and the outcomes of this study are graphically presented in Fig. 12 **(b)** $\left(\ln\left(\frac{A_0}{A_t}\right)\right.$ versus time) at 3 ml catalyst. Consequently, we assessed the rate constant governing the degradation of MB dye by Cu-Ag-BMNPs, employing the pseudo-first-order kinetics model. Notably, the slope rate constant exhibited a higher value ($R^2 = 97.8$ for the 3 ml and $R^2 = 97.8$ for the 5 ml) Cu-Ag-BMNPs catalyst in comparison to the 5 ml catalyst concentration. The inclination of this line, which defines the fitting, acts as a key indicator for the rate constant associated with the green synthesis of Cu-Ag-BMNPs. When exposed to visible light, the phytochemicals found in the AN extract played a pivotal role in facilitating the transfer of electrons from the valence band to the conduction band of the Cu-Ag-BMNPs composite. This phenomenon resulted in an increased generation of superoxide radicals, ultimately enhancing the overall efficiency of the photo-degradation process catalyzed by Cu-Ag-BMNPs. These insights shed light on the intricate mechanisms governing the photo-catalytic activity of Cu-Ag-BMNPs, highlighting their potential for advanced environmental applications [50–54].

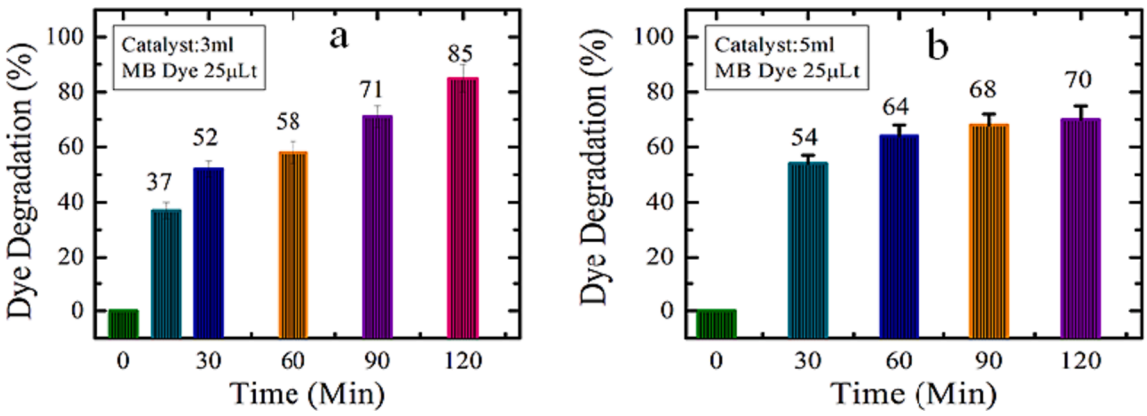

Fig. 11. Dye degradation of MB dye as the function time (Min) at (a) 3 ml, (b) 5 ml catalyst concentration.

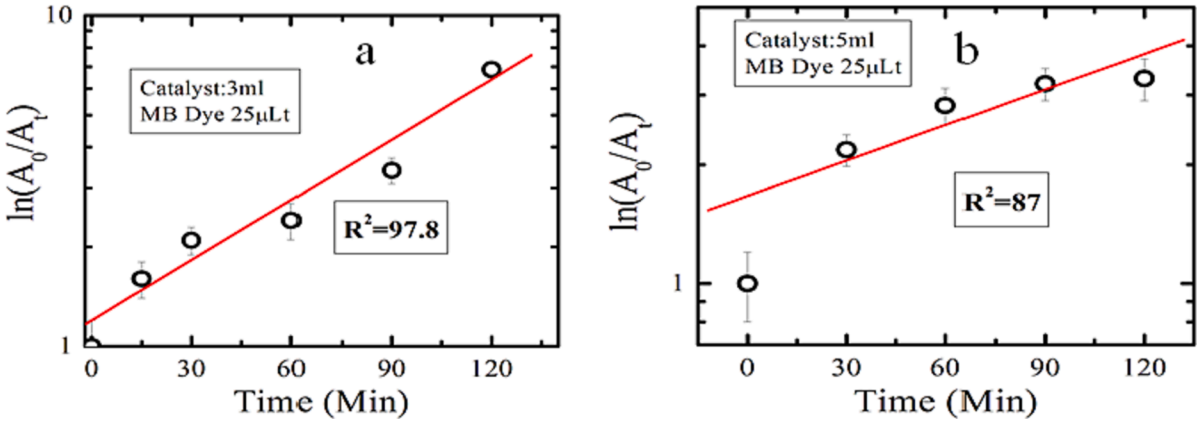

Fig. 12. Kinetic results for dye degradation: (lnA_t/A_0) vs Time at (a) 3 ml, (b) 5 ml catalyst.

3.5.2. *Possible mechanism of Cu-Ag-BMNPs*

The core entities engaged in the detoxification of MB dye molecules under light were elucidated via the process of photo-catalysis. Fig. 13 provides a clear illustration of the proposed mechanism that governs the photo-catalytic degradation of dye. MNPs/BMNPs with a narrow band gap serve as a crucial catalyst in promoting the generation of electron-hole pairs. This is due to the minimal absorption energy required for electrons to transition from the higher occupied orbit states to the lower unoccupied orbit state. Upon absorbing light energy, a catalyst such as Cu-Ag-BMNPs exhibits an absorption intensity that aligns with the band

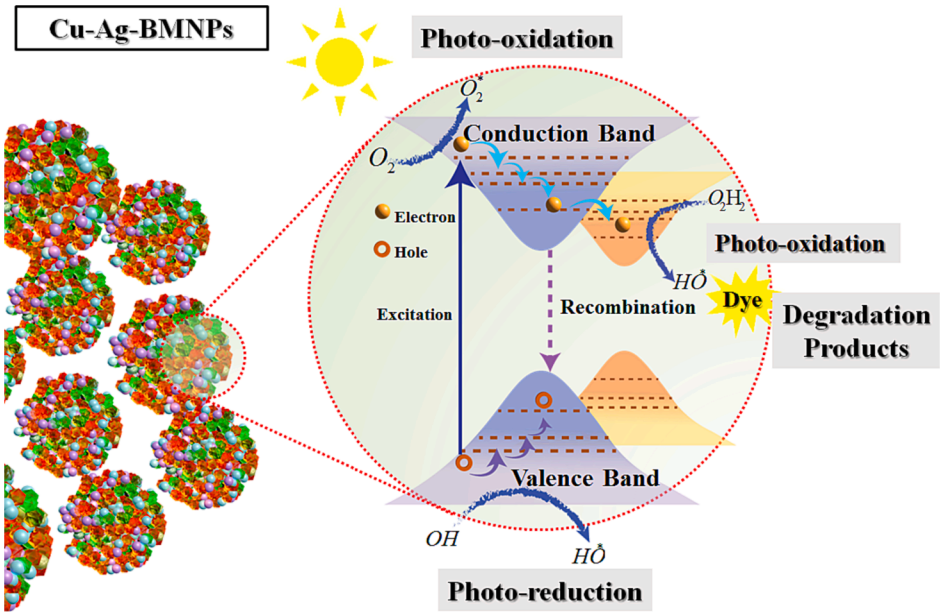

Fig. 13. Schematic representation of photo-catalytic mechanism.

gap energy of the catalyst itself. The process of energy transition entails a shift from the ground state to the excited state, resulting in the emergence of several critical components, including a band gap, a valence band hole, h^+, a liberated electron, and a conduction band electron, e^-. Remarkably, the hole plays a pivotal role as an attractive receptor for electrons from pollutants, thereby initiating their degradation. In this intricate process, highly oxidizing species come into play, converting water molecules into hydroxyl radicals (OH), which play a pivotal role in degrading organic contaminants. Concurrently, oxygen molecules combine with electrons, transforming into superoxide radicals (O2). The reduction of pollutants unfolds through the following sequence

$$\text{Photcatalyst CuO} + h\nu \rightarrow e^- + h^+$$

$$\text{Photcatalyst CuO}(e^-) + h\nu \rightarrow O_2^-$$

$$\text{Photcatalyst CuO}(h^+) + H_2O \rightarrow OH^-$$

$$O_2^-(or)OH^- + Dye \rightarrow \text{Degraded material}$$

This elucidation provides valuable insights into the intricate pathways through which pollutants are effectively reduced, shedding light on the promising potential of these mechanisms in advanced environmental applications.

The surface of Cu-Ag-BMNPs was adorned with phenolic compounds and bio-flavonoids derived from the AN extract. These phytochemical constituents play a pivotal role in augmenting the generation of superoxide radicals from oxygen molecules, thereby enhancing the overall photo-catalytic activity. Importantly, our findings confirm that oxide and hydroxyl radicals are indeed the predominant reactive species generated during the photocatalytic degradation of water-soluble dyes. This insight adds depth to our understanding of the mechanistic intricacies underlying the photo-catalysis process, underscoring the potential of Cu-Ag-BMNPs for advanced applications in the realm of environmental remediation.

3.5.3. Factors affecting photocatalytic degradation of Cu-Ag-BMNPs

To attain optimal photo-catalytic activity, several critical factors necessitate consideration, including dye concentration, photo-catalyst concentration, catalyst structure and morphology, irradiation duration, and the light source employed. Notably, an inhibitory effect is observed when the dye concentration is increased, primarily due to the diminished interaction with the active sites of the catalyst. This phenomenon arises from the reduced light absorption capacity of dye molecules at higher concentrations, hindering the migration of electrons to the photo-catalyst. Consequently, an insufficient quantity of hydroxyl radicals is generated for effective dye degradation, thereby diminishing the overall efficiency of the degradation process. Our findings highlight the efficacy of a 1 mg/lit concentration of MB dye solution in achieving superior results in this context.

As the concentration of the photo-catalyst increases or at optimum concentration (3 ml), there is a corresponding increase in the number of available reaction sites, which in turn leads to the enhanced generation of electron-hole pairs. Consequently, this promotes the amplified production of hydroxyl radicals, which are indispensable for the efficient detoxification of organic pollutants. Additionally, it's worth highlighting that the morphological characteristics and grain size of Cu-Ag-BMNPs are pivotal factors affecting the efficacy of MB dye degradation. Catalyst nanoparticles with smaller sizes exhibit enhanced efficiency in dye degradation due to their ability to provide a higher quantity of active sites for dye absorption. In our investigations, we achieved noteworthy results by employing a 3 ml Cu-Ag-BMNPs catalyst in comparison to a 5 ml catalyst, with both utilizing the same concentration of MB dyeAn impressive degradation rate of 85 % for MB dye was achieved within a 120-minute time interval using a 3 ml concentration of Cu-Ag-BMNPs catalyst. It's worth emphasizing that our Cu-Ag-BMNPs catalyst was synthesized through a straightforward and environmentally friendly green synthesis process, utilizing AN leaf extract. This synthesis process demonstrated remarkable efficiency, achieving an 85 % degradation rate for MB under standard visible light conditions. These results underscore the significant potential of Cu-Ag-BMNPs as highly effective catalysts in various environmental applications.

4. Conclusion

In conclusion, the green-synthesized Cu-Ag-BMNPs showcase significant potential as efficient photo-catalysts for combatting water pollution, particularly at an optimum catalyst concentration of 3 ml. Demonstrating an impressive 85 % dye degradation rate, these nanoparticles prove effective in removing harmful organic contaminants under environmentally friendly conditions. Achieving optimal photocatalytic activity requires careful consideration of various factors, including dye and catalyst concentrations, catalyst structure, irradiation duration, and the light source used. The kinetics of MB dye degradation, modeled using the first-order kinetic theory, provide valuable insights. Future research endeavors should prioritize the optimization of catalyst and dye concentrations, delve into the intricacies of photo-catalytic mechanisms, conduct thorough toxicity evaluations, and assess sustained performance in real-world scenarios. The environmentally conscious green synthesis approach, minimizing the use of hazardous chemicals, underscores a commitment to sustainable practices. These collective efforts pave the way for scalable industrial production, ultimately contributing significantly to both human health and the global environment.

5. Data availabilit y

Data is provided with the request.

Ethical approval

Internal review board committee of our lab state that we do not have any consent to publish this antimicrobial and other data.

No funding was received for this project.

CRediT authorship contribution statement

Parvathalu Kalakonda: Conceptualization, Project administration, Supervision, Writing – original draft, Writing – review & editing. **Anusha Bashitangu:** Data curation, Investigation, Methodology. **Pritam Mandal:** Formal analysis, Investigation. **Sarvani Jowhar Khanam:** Data curation, Investigation. **Murali Banovath:** Formal analysis. **Imran Hasan:** Formal analysis. **Bala Bhaskar Podila:** .

Declaration of competing interest

The authors declare that they have no known competing financial interests or personal relationships that could have appeared to influence the work reported in this paper.

Data availability

Data will be made available on request.

Acknowledgement

1. The authors extend their thanks to Government City College (Autonomous) and Department of Chemistry, University of Hyderabad for supporting basic facilities and characterization of materials.

2. The authors extend their thanks to Researchers supporting Project (Ref:RSPD2023R670), King Saud University, Riyadh, KSA.

References

[1] M.F. Hanafi, N. Sapawe, A review on the water problem associate with organic pollutants derived from phenol, methyl orange, and remazol brilliant blue dyes, Mater. Today Proc. 31 (2020) 141–150.

[2] T. Islam, M. Repon, T. Islam, et al., Impact of textile dyes on health and ecosystem: a review of structure, causes, and potential solutions, Environ Sci Pollut Res 30 (2023) 9207–9242.

[3] K.G. Pavithra, V. Jaikumar, Removal of colorants from wastewater: A review on sources and treatment strategies, J. Ind. Eng. Chem. 75 (2019) 1–19.

[4] M. Ismail, K. Akhtar, M. Khan, T. Kamal, M.A. Khan, M.A. Asiri, J. Seo, S.B. Khan, Pollution, toxicity and carcinogenicity of organic dyes and their catalytic bio-remediation, Curr. Pharm. Des. 25 (2019) 36453–36663.

[5] S. Rana, S. Handa, Y. Aggarwal, S. Puri, M. Chatterjee, Role of Candida in the bioremediation of pollutants: a review, Letters in Applied Microbiology, Volume 76, Issue 9, September 2023;9,76;1-9.

[6] D.J. Patil, S.N. Behera, Synthesis and characterization of nanoparticles of cobalt and nickel ferrites for elimination of hazardous organic dyes from industrial wastewater, Environ Sci Pollut Res. 30 (2023) 53323–53338.

[7] P.K. Elumalai, G.P. Selvan, et al., Review on heavy metal contaminants in freshwater fish in South India: current situation and future perspective, Environ Sci Pollut Res (2023).

[8] K. Naseem, R. Begum, W. Wu, A. Irfan, A.G. Al-Sehemi, Z.H. Farooqi, Catalytic reduction of toxic dyes in the presence of silver nanoparticles impregnated core-shell composite microgels, J. Clean. Prod. b211 (2019) 855–864.

[9] S. Daniel, P.S. Syed, Shabudeen Sequestration of carcinogenic dye in waste water by utilizing an encapsulated activated carbon with nano MgO, Int. J. Chemtech Res. 7 (2014) 2235–2243.

[10] S. Vasantharaj, S. Sathiyavimal, M. Saravanan, P. Senthilkumar, K. Gnanasekaran, M. Shanmugavel, A. Pugazhendhi, Synthesis of ecofriendly copper oxide nanoparticles for fabrication over textile fabrics: characterization of antibacterial activity and dye degradation potential, J. Photochem. Photobiol. B Biol. 191 (2019) 143–149.

[11] C.V. Reddy, K.R. Reddy, V.A. Harish, J. Shim, M. Shankar, N.P. Shetti, T. M. Aminabhavi, Metal-organic frameworks (MOFs)- based efficient heterogeneous photo-catalysts: Synthesis, properties and its applications in photocatalytic hydrogen generation, CO2 reduction and photodegradation of organic dyes, Int. J. Hydrog. Energy 45 (2020) 7656–7679.

[12] S. Khan, U. Bhardwaj, H.M. Iqbal, N. Joshi, Synergistic role of bacterial consortium to biodegrade toxic dyes containing wastewater and its simultaneous reuse as an added value, Chemosphere 284 (2021), 131273.

[13] A. Ahmad, S.H. Mohd-Setapar, C.S. Chuong, A. Khatoon, W.A. Wani, R. Kumar, M. Rafatullah, Recent advances in new generation dye removal technologies: Novel search for approaches to reprocess wastewater, RSC Adv. 5 (2015) 30801–30818.

[14] T. Adane, A.T. Adugna, E. Alemayehu, Textile industry effluent treatment techniques, J. Chem. 5314404 (2021) 1–14.

[15] S. Rao, S. AS, G.K. Jayaprakash, M.M. Swamy, K S, D. Kumar, Plant seed extract assisted, eco-synthesized C-ZnO nanoparticles: Characterization, chromium(VI) ion adsorption and kinetic studies, Luminescence (2022).

[16] A. Ahmed, M. Usman, B. Yu, X. Ding, Q. Peng, Y. Shen, H. Cong, Efficient photocatalytic degradation of toxic Alizarin yellow R dye from industrial wastewater using biosynthesized Fe nanoparticle and study of factors affecting the degradation rate, J. Photochem. Photobiol. B Biol. 202 (2020), 111682.

[20] S. Aroob, M.B. Taj, S. Shabbir, M. Imran, R.H. Ahmad, S. Habib, A. Raheel, M. N. Akhtar, M. Ashfaq, M. Sillanpää, In situ biogenic synthesis of CuO nanoparticles over graphene oxide: A potential nanohybrid for water treatment, J. Environ. Chem. Eng. 9 (2021), 105590.

[21] M. Mitra, S.T. Ahamed, A. Ghosh, A. Mondal, K. Kargupta, S. Ganguly, D. Banerjee, Polyaniline/reduced grapheme oxide composite-enhanced visible-light-driven photocatalytic activity for the degradation of organic dyes, ACS Omega 4 (2019) 1623–1635.

[22] S. Feng, F. Li, Photocatalytic dyes degradation on suspended and cement paste immobilized TiO2/g-C3N4 under simulated solar light, J. Environ. Chem. Eng. 9 (2021), 105488.

[23] C. Karthikeyan, P. Arunachalam, K. Ramachandran, A.M. Al-Mayouf, S. Karuppuchamy, Recent advances in semiconductor metal oxides with enhanced methods for solar photocatalytic applications, J. Alloy. Compd. 828 (2020), 154281.

[24] Ta¸sdemïrcï, t.ç., Synthesis of copper-doped nickel oxide thin films: Structural and optical studies, Chem. Phys. Lett. (2020) 738,136884.

[25] P. Kalakonda, Synthesis of silver nanowires for highly conductive and transparent films, Nanomater. Nanotechnol. (2016) 6.

[26] P. Kalakonda, B. Sreenivas, Synthesis and Optical Properties of Highly Stabilized Peptide-Coated Gold Nanoparticles, Plasmonics 12 (2017) 1221–1225.

[27] T. Naseem, T. Durrani, The role of some important metal oxide nanoparticles for wastewater and antibacterial applications: A review, Environ. Chem. Ecotoxicol. 3 (2021) 59–75.

[28] S. Pourmoslemi, N. Bayati, R. Mahjub, Application of Box-Behnken design to optimize a sol-gel synthesis method for Ag and Zn doped CuO nanoparticles with antibacterial and photocatalytic activity, J. Sol-Gel Sci. Technol. 104 (2022) 319–329.

[29] T. Elysabeth, K. Mulia, M. Ibadurrohman, E.L. Dewi, A comparative study of CuO deposition methods on titania nanotube arrays for photoelectrocatalytic ammonia degradation and hydrogen production, Int. J. Hydrog. Energy 46 (2021) 26873–26885.

[30] S.M. Ahmad, et al., Phylogenetic patterns and genetic diversity of Indian Tinospora species based on chloroplast sequence data and cytochrome P450 polymorphisms, Plant Syst. Evol. 281 (2009) 87–96.

[31] J.G. Asthana, et al., Evaluation of antileprosy herbal drug combinations and their combinations with dapsone, INDIAN DRUGS-BOMBAY 38 (2) (2001) 82–86.

[34] Prince, P.S. Mainzen, V.P. Menon, Antioxidant activity of Tinospora cordifolia roots in experimental diabetes, J. Ethnopharmacol. 65 (3) (1999) 277–281.

[35] K. Parvathalu, D.N. Kumar, K. Rajitha, et al., Facile Synthesis of Silver Nanoparticles Using Green Tea Leaf Extract and Evolution of Antibacterial Activity, Plasmonics (2023), https://doi.org/10.1007/s11468-023-01899-6.

[36] K. Parvathalu, S. Chinmayee, B. Preethi, et al., Green Synthesis of Silver Nanoparticles Using *Argyreia nervosa* Leaf Extract and Their Antimicrobial Activity, Plasmonics 18 (2023) 1075–1081.

[37] P. Sharma, S. Pant, P. Poonia, et al., Green Synthesis of Colloidal Copper Nanoparticles Capped with *Tinospora cordifolia* and Its Application in Catalytic Degradation in Textile Dye: An Ecologically Sound Approach, J Inorg Organomet Polym 28 (2018) 2463–2472.

[38] P.C. Udayabhanu, M.A.P. Nethravathi, D. Kumar, K. Suresh, H. Lingaraju, H. Rajanaika, S.C.S. Nagabhushana, Tinospora cordifolia mediated facile green synthesis of cupric oxide nanoparticles and their photocatalytic, antioxidant and antibacterial properties, Mater. Sci. Semicond. Process. 33 (2015) 81–88.

[39] K. Selvam, C. Sudhakar, M. Govarthanan, P. Thiyagarajan, A. Sengottaiyan, Balakrishnan Senthilkumar, Thangasamy Selvankumar, Eco-friendly biosynthesis and characterization of silver nanoparticles using Tinospora cordifolia (Thunb.) Miers and evaluate its antibacterial, antioxidant potential, Journal of Radiation Research and Applied Sciences 10 (2017) 6–12.

[40] L. Chompunut, T. Wanaporn, W. Anupong, M. Narayanan, M.h. Alshiekheid, A. Sabour, I. Karuppusamy, N.T.L. Chi, R. Shanmuganathan, Synthesis of copper nanoparticles from the aqueous extract of Cynodon dactylon and evaluation of its antimicrobial and photocatalytic properties, Food Chem. Toxicol. 166 (2022), 113245.

[41] P. Munnik, P.E. De Jongh, K.P. De Jong, Recent developments in the synthesis of supported catalysts, Chem. Rev. 115 (2015) 6687–6718.

[42] F. Schüth, Control of solid catalysts down to the atomic scale: Where is the limit Angew, Chem. Int. Ed. 53 (2014) 8599–8604.

[43] F. Schüth, Strukturierung fester Katalysatoren bis hinab zur atomaren Skala: Wo liegen die Grenzen Angew, Chem 126 (2014) 8741–8747.

[44] P. Kalakonda, Synthesis of silver nanowires for highly conductive and transparent films, Nanomater. Nanotechnol. 6 (2016).

[45] P. Kalakonda, S. Banne, Synthesis and Optical Properties of Highly Stabilized Peptide-Coated Silver Nanoparticles, Plasmonics 13 (4) (2018) 1265–1269.

[46] P. Kalakonda, et al., Microfibrous silver-coated polymeric scaffolds with tunable mechanical properties, RSC Adv. 7 (55) (2017) 34331–34338.

[47] K. Parvathalu, et al., Facile Synthesis of Silver Nanoparticles Using Green Tea Leaf Extract and Evolution of Antibacterial Activity, Plasmonics (2023).

[48] E.A. Mohamed, Green synthesis of copper & copper oxide nanoparticles using the extract of seedless dates, Heliyon 6 (1) (2020) e03123.

[49] K. Parvathalu, K. Rajitha, B. Chandrashekar, et al., Biomimetic Synthesis of Copper Nanoparticles Using Tinospora Cordifolia Plant Leaf Extract for Photocatalytic Activity Applications, Plasmonics (2023).

[50] A. Velidandi, N.P. Pabbathi, S. Dahariya, R.R. Baadhe, Green synthesis of novel Ag-Cu and Ag-Znbimetallic nanoparticles and their in vitro biological, eco-toxicity and catalytic studies, Nano-Structures & Nano-Objects. 26 (2021), 100687.

[51] M.A. Malik, S.S. Albeladi, S.M. Al-Maaqar, A.A. Alshehri, S.A. Al-Thabaiti, I. Khan, M.R. Kamli, Biosynthesis of Novel Ag-Cu Bimetallic Nanoparticles from Leaf Extract of Salvia officinalis and Their Antibacterial Activity, Life. 13 (3) (2023) 653.

[52] G. Mamatha, P. Sowmya, D. Madhuri, N. Mohan Babu, D. Suresh Kumar, G. Vijaya Charan, K. Varaprasad, K. Madhukar, Antimicrobial cellulose nanocomposite films with in situ generations of bimetallic (Ag and Cu) nanoparticles using Vitex negundo leaves extract, J. Inorg. Organomet. Polym Mater. 31 (2021) 802–815.

[53] H. Babu, M.M. Kareem, L.GV. Photocatalytic, antioxidant and biological activities of Alternantherasessilis (Linn.) leaf aqueous extract mediated Ag-Cu bimetallic nanoparticles, Mater. Today:. Proc. (2023).

[54] P.B. Ashishie, C.A. Anyama, A.A. Ayi, C.O. Oseghale, E.T. Adesuji, A.H. Labulo, Green synthesis of silver monometallic and copper-silver bimetallic nanoparticles using Kigelia africana fruit extract and evaluation of their antimicrobial activities, International Journal of Physical Sciences. 13 (3) (2018) 24–32.